EFFECT OF INTERNAL DIFFUSION ON CATALYTIC REACTIONS. XI.*
HYDROGENOLYSIS OF CYCLOPROPANE ON A PALLADIUM/ALUMINA CATALYST

L. ANTL and P. SCHNEIDER

Institute of Chemical Process Fundamentals,
Czechoslovak Academy of Sciences, 165 02 Prague - Suchdol

Received December 8th, 1972

The differential mass balance equations were derived for a catalytic reaction governed by an arbitrary kinetic equation in a catalyst pellet. The multicomponent diffusion in the transition region was described alternatively by the diffusion equation (*2*) (model I) or simple Fick's equation (*3*) (model II). The diffusion equations provide also mutual concentrations of individual species in the reaction mixture in a given position in the pellet and the conditions of a proper selection of the key (balanced) species. The effective reaction rates and the effectiveness factors of hydrogenolysis of cyclopropane on cylindrical Pd/Al_2O_3 catalyst pellets were measured in a circulating differential reactor at 20 and 40°C. The experimental data were used to determine the geometrical factor of the pellet based on model I and II. It turns out that model I is somewhat superior to model II and that the mean pore radius, determined as an integral mean of the frequency curve of the pore distribution, provides more consistent results than the Wheeler radius.

Although in the majority of real catalytic reactions diffusion takes place in the transition region and the reaction mixture is often multicomponent, the attention has been focused predominatly on cases where either the reaction rate depends on concentration of a single species, or, the diffusion is described by a simple form of the Fick law (the Knudsen or molecular diffusion). In this paper we have applied alternatively two models of the multicomponent reaction in the transition region of diffusion and compared them with experimental results. As a model reaction we took hydrogenolysis of cyclopropane which proceeds on the Pd/Al_2O_3 catalyst quite selectively giving rise to a single product – propane. The kinetics of this reaction can be studied at temperatures close to the room temperature[1].

THEORETICAL

Diffusion equation. In the derivation we shall assume that for the model reaction

$$\sum_i \alpha_i A_i = 0 \quad (i = 1, \ldots, p) \qquad (1)$$

* Part X: This Journal *37*, 2507 (1972).

the true porous structure of the catalyst can be replaced by a pseudo-homogeneous structure. In addition to the reacting species $i = 1, \ldots, p$ the mixture may contain also inert components ($i = q, \ldots, n$). Two alternative equations shall be considered to express the diffusion flux of the species A_i in a multicomponent mixture

$$N_i = -D_i c_T \nabla y_i + y_i \sum N_j \quad (j = 1, \ldots, n) \tag{2}$$

analogous to the relation for a binary mixture and

$$N_i = -D_i c_T \nabla y_i \tag{3}$$

formally identical to the Fick law. The effective diffusion coefficients, D_i, defined by Eqs (2) and (3), include a geometrical factor ε/q (porosity/tortuosity) to account for the fact that the pores represent only a fraction of the cross-section of the porous structure, and, further, that the pores are generally longer than the dimension of the pellet. The diffusion characteristic proper is then the coefficient $\mathscr{D}_i$

$$D_i = (\varepsilon/q)\,\mathscr{D}_i \tag{4}$$

which may be viewed as a diffusion coefficient of the species A_i in a multicomponent gas mixture. For isobaric diffusion of the species A_i in a multicomponent gas mixture in the transition region of diffusion one can write[2-5] a relation analogous to the Stefan–Maxwell equation which in an one-dimensional case has the form

$$-c_T(\mathrm{d}y_i/\mathrm{d}x) = [N_i/(\varepsilon/q)\,\mathscr{D}_{ki}] + \sum_{j=1}^{n} [1/(\varepsilon/q)\,\mathscr{D}_{ij}]\,(y_j N_i - y_i N_j)\,. \tag{5}$$

The binary diffusion coefficient of the pair A_i—A_j, $\mathscr{D}_{ij}$, is assumed to be concentration-independent. The Knudsen diffusion coefficient of the species A_i in a circular pore of radius r is given by

$$\mathscr{D}_{ki} = (2/3) r v_i\,. \tag{6}$$

For stoichiometry reasons the diffusion fluxes are related by

$$N_i/\alpha_i = \text{const.} \quad (i = 1, \ldots, p)\,. \tag{7}$$

For the inert species we have clearly

$$N_i = 0 \quad (i = q, \ldots, n)\,. \tag{8}$$

With the aid of the stoichiometry coefficients

$$a_i = \alpha_i/\alpha_1 , \tag{9}$$

the diffusion flux of an arbitrary species can be expressed in terms of the flux of the key species A_1

$$N_i = a_i N_1 \quad (i = 1, \ldots, p) . \tag{10}$$

Combining Eqs (5), (8) and (10) we get

$$-(\varepsilon/q)\, c_T(\mathrm{d}y_i/\mathrm{d}x) = N_1[a_i/\mathscr{D}_{ki} + \sum_{j=1}^{p}(y_j a_i - y_i a_j)/\mathscr{D}_{ij} + a_i \sum_{j=q}^{n} y_j/\mathscr{D}_{ij}] \quad i = 1, \ldots, n, \tag{11}$$

where for inert species by definition $a_i = 0$ $(i = q, \ldots n)$. Combining Eq. (11) with Eq. (2) and using relations (7) and (8) we get for the diffusion coefficient of species A_i in the multicomponent mixture in the transition region

$$\mathscr{D}_i = (a_i - a y_i)/[a_i/\mathscr{D}_{ki} + \sum_{j=1}^{n}(y_j a_i - y_i a_j)/\mathscr{D}_{ij} + a_i \sum_{j=q}^{p} y_j \mathscr{D}_{ij}] \quad i = 1, \ldots, n , \tag{12}$$

where

$$a = \sum_{j=1}^{p} a_i \tag{13}$$

is the change of the mole number due to reaction. As it is apparent from Eq. (12), the diffusion coefficient $\mathscr{D}_i$ (and hereby D_i, see Eq. (4)) depends on composition of the reaction mixture and thus on the position within the catalyst. Since the differential mass balances assume constant diffusion coefficient within the whole volume of the pellet, some average value of this coefficient must be used. For simplicity we shall assume the concentration dependence of the diffusion coefficient along the pore to be weak and replace the average by the value on the outer surface (subscript s) of the pellet: $\mathscr{D}_{is} = \mathscr{D}_i(y_{js})$, or $D_{is} = D_i(y_{js})$.

Relations between concentrations within the pellet. The reaction rate in the balance must be expressed in terms of concentration of the balanced (key) species. Thus the relations are needed between concentrations of individual species appearing in the reaction rate term, and the concentration of the balanced (key) species in a given position within the pellet. Combining the diffusion equation (2) for the i-th species with that for the key species $(i = 1)$ and using the stoichiometry relations (10) we arrive at the following differential equation relating the mole fractions of both species $y_i = y_i(y_1)$

$$\mathrm{d}y_i/\mathrm{d}x = [(a_i - a y_i)/(1 - a y_1)]\,(D_1/D_i) , \qquad i = 1, \ldots, p . \tag{14}$$

On integrating the last differential equation together with the boundary conditions fixing the mixture composition at the outer surface (for $y_1 = y_{1s}$, $y_i = y_{is}$) and assuming the ratio of the diffusion coefficients D_1/D_i to be concentration-independent, the concentration relations of the type $y_i = y_i(y_1)$ are obtained

$$y_i = (a_i/a)\left\{1 - \left[1 - (ay_{is}/a_i)\right]\left[(1 - ay_1)/(1 - ay_{1s})\right]^{D_1/D_1}\right\}, \quad i = 1, \ldots, p. \tag{15}$$

Considering that the stoichiometry coefficients a_i of the inerts ($i = q, \ldots, n$) equal zero, Eq. (15) can be simplified to give

$$y_i = y_{is}\left[(1 - ay_1)/(1 - ay_{1s})\right]^{D_1/D_1}, \qquad i = q, \ldots, n. \tag{16}$$

In a similar way leading to Eqs (15) and (16) from Eq. (2), one can obtain from Eq. (3) the following relations

$$y_i = y_{is} - (a_i D_1/D_i)(y_{1s} - y_1), \qquad i = 1, \ldots, p. \tag{17}$$

For inert species ($a_i = 0$) we find easily that $y_i = y_{is}$ ($i = q, \ldots, n$). While the diffusion equation (3) leads to a linear expression between the concentrations (Eq. (17)), an analogous expression based on the diffusion equation (2) is a non-linear one (Eq. (15)).

The choice of the key component. The choice of the key species for a multicomponent reaction with several reactants may not be quite straightforward. For a bimolecular reaction $aA + bB = \ldots$, for instance, one can take for A_1 either A or B. In diffusion problems in porous catalysts this arbitrariness is somewhat limited by the requirement that the mole fractions (concentrations, partial pressures) of the remaining reactants ("non-key species") must not take negative values. Since the mole fractions of all reactants decrease toward the pellet center, it is necessary that in a position where the concentration of the key species vanishes the concentrations of the remaining reactants must satisfy the constraint $y_i \geqq 0$ ($i = 2, \ldots, k$, where k is a subscript of the last reactant A_k). On implementing this stipulation in the relations for mole fractions of the reactions species (Eq. (15) or (17)) one can formulate necessary conditions for proper choice of the key species. In case of non-linear relations between concentrations (Eq. (15)) and reactions with an increase in the mole number ($a < 0$), a proper choice is indicated by the following nonequality containing the ratio of the diffusion coefficient and the stoichiometry coefficients

$$(1 - ay_{1s})^{D_1/D_1} \leqq 1 - (a/a_i)\, y_{is} \quad (i = 2, \ldots, k). \tag{18}$$

For a reaction with a decrease in the mole number ($a > 0$) this condition takes the form

$$(1 - a y_{1s})^{D_1/D_i} \geqq 1 - (a/a_i)\, y_{is} \quad (i = 2, \ldots, k)\,. \tag{19}$$

In order that the exponentiation to a rational positive exponent D_1/D_i be defined one must have necessarily $1 - a y_{1s} \geqq 0$.

When using linear relations between concentrations (Eq. (17)) the necessary condition of a proper choice of the key species is then

$$y_{is}/y_{1s} \geqq a_i D_1/D_i\,, \quad (i = 2, \ldots, k)\,. \tag{20}$$

The mass balance for an isothermal catalyst pellet. The mass balance on the key species A_1 in a one-dimensional catalyst pellet (infinite slab $w = 0$, infinite cylinder $w = 1$, sphere $w = 2$) may be written as

$$(1/z^w)\,(\mathrm{d}/\mathrm{d}z)\,(-z^w N_1) = R_1\,. \tag{21}$$

When using Eq. (2) for the diffusion flux N_1 the differential mass balance (model I) has the form

$$\frac{\mathrm{d}^2 c}{\mathrm{d}x^2} + \frac{\mathrm{d}c}{\mathrm{d}x}\left[\frac{w}{x} + \frac{H}{1 - Hc}\frac{\mathrm{d}c}{\mathrm{d}x}\right] = M_w^2(1 - Hc)\,\mathrm{f}(c)\,. \tag{22}$$

The dimensionless concentration of the key species, c, is defined as $c = y_1/y_{1s}$; the dimensionless coordinate x so as to have $x = 0$ in the center and $x = 1$ on the surface of the pellet. The dimensionless reaction rate, $\mathrm{f}(c)$, is related to the rate on the pellet surface (R_{1s}), by $\mathrm{f}(c) = R_1(c)/R_{1s}$. The parameters M_w and H are defined as follows

$$M_w^2 = l_w^2(R_{1s}/D_1 y_{1s} c_T)\,, \qquad (w = 0, 1, 2) \tag{23}$$

$$H = a y_{1s}\,. \tag{24}$$

In case of the catalyst pellet forming a slab, the characteristic dimension, l_0, appearing in the Thiele modulus, equals one half of the slab thickness; for an infinite cylinder l_1 is its radius; for a sphere l_2 is its radius.

The boundary conditions pertaining to Eq. (22) have a familiar form

$$x = 0 \qquad c = 1\,, \tag{25}$$

$$x = 1 \qquad \mathrm{d}c/\mathrm{d}x = 0\,. \tag{26}$$

The parameter H appearing in Eq. (22) characterizes the effect of the change of the number of moles due to reaction. Its value is affected both by the change of the number of moles and the concentration of the key species on the outer surface of the pellet (y_{1s}). (The same parameter has been used *e.g.* by Weekmann and Gorring[6].) As a condition for the existence of exponentiation to D_1/D_i we found in connection with Eqs (18) and (19) that $1 - H \geqq 0$. Since $a > 0$ for reactions with a decrease in the mole number, H must be in the interval $0 \leqq H \leqq 1$. For reactions with an increase in the mole number $a < 0$ and H is therefore delimited by $H \leqq 0$.

If one uses Eq. (3) to define the diffusion flux in the mass balance (21) the following differential equation (model II) is obtained

$$d^2c/dx^2 + (w/x)\, dc/dx = M_w^2 f(c), \tag{27}$$

where w, M_w and $f(c)$ have the same meaning as those in Eq. (22). The boundary conditions (25) and (26) remain also unchanged. It is seen that Eq. (27) is a special case of Eq. (22) for $H \to 0$, *i.e.* for a reaction with no change in the mole number.

The effectiveness factor. The effectiveness factor, η_w, is currently defined as a ratio of the amount of the key species penetrating in the pellet through the outer surface to react to that which would react in the absence of the diffusion effects. From the diffusion equation (2) and the definition one can arrive at the following expression (model I) for the effectiveness factor

$$\eta_w = [(w + 1)/M_w^2]\,[-c'(1)/(1 - H)]. \tag{28}$$

This equation enables the effectiveness factor to be determined from the gradient of the dimensionless concentration of the key species at the outer surface of the pellet, $c'(1)$. Using Eq. (3) the expression for the effectiveness factor takes the form (model II)

$$\eta_w = [(w + 1)/M_w^2]\,[-c'(1)], \tag{29}$$

which is a limiting expression of Eq. (28) for $H \to 0$. In case of a strong diffusion effect the boundary condition (26) for an irreversible reaction can be replaced to a fair approximation by

$$x = 1, \qquad c = 0. \tag{30}$$

The approximation is the better the higher the value of the modulus M_w. For a high value of the modulus one can further simplify the balance equations (22) and (27). Substituting *e.g.* $v = M_w(1 - x)$, Eq. (22) takes the form

$$\frac{d^2c}{dv^2} + \frac{w}{(M_w - v)}\frac{dc}{dv} + \frac{H}{1 - Hc}\left(\frac{dc}{dv}\right)^2 = (1 - Hc)\, f(c). \tag{31}$$

(Eq. (27) changes by this substitution into one obtained from Eq. (31) by the limit $H \to 0$). For high values of the modulus M_w the second term on the left hand side of Eq. (31) may be neglected and in region of strong diffusion effect (asymptotic region) there results after changing over to x (model I)

$$\frac{d^2c}{dx^2} + \frac{H}{1 - Hc}\left(\frac{dc}{dx}\right)^2 = M_w^2(1 - Hc)\,f(c) \qquad (32)$$

For $H \to 0$ Eq. (31) gives

$$d^2c/dx^2 = M_w^2\,f(c)\,, \qquad (33)$$

which describes the diffusion effect in region of strong inner diffusion provided that the diffusion flux is given by Eq. (3) (model II).

Eqs (32) and (33), excepting the definition of M_w, are identical to the balance equations for a slab. The cause is that under strong effect of internal diffusion the reaction takes place only within a thin shell below the outer surface of the pellet. The thinner the shell relatively to the pellet diameter the better the approximation of the pellet geometry to an infinite slab, for which we have Eq. (22) or (27) with $w = 0$. Substituting $p = dc/dx$ the differential equations (32) and (33) can be transformed into a linear differential equation of the first order and integrated analytically. With the aid of the boundary conditions (25) and (30) one can obtain an expression for the gradients of the relative mole fraction of the key species on the outer surface of the pellet, $c'(1)$ necessary to evaluate the effectiveness factor from Eqs (28) and (29). For the diffusion equation (2) the effectiveness factor in region of strong internal diffusion, η_w^*, is given (model I) as

$$\eta_w^* = \frac{w + 1}{M_w}\sqrt{\left(\left[2\int_0^1 \frac{f(c)\,dc}{1 - Hc}\right]\right)}. \qquad (34)$$

With the diffusion being described by Eq. (3) the expression for the effectivenes factor (model II) takes the form

$$\eta_w^* = \frac{w + 1}{M_w}\sqrt{\left(\left[2\int_0^1 f(c)\,dc\right]\right)}. \qquad (35)$$

Similarly as in the preceding equations, Eq. (35) is a special case of Eq. (34) for $H \to 0$.

The kinetics of hydrogenolysis of cyclopropane. The kinetics of the selective hydrogenolysis of cyclopropane to propane on a Pd/Al_2O_3 catalyst has been studied

recently in this laboratory[1,7] on the same catalyst as that used in this work. The best kinetic equation found by nonlinear regression of the experimental data at 20°C was

$$R_A = k\sqrt{(K_A K_B p_A p_B)}/(1 + \sqrt{(K_A p_A)} + \sqrt{(K_B p_B)} + K_C p_C)^2 \qquad (36)$$

(A cyclopropane, B hydrogen, C propane, $k = 46{\cdot}6$ mol/h kg_{cat}, $K_A = 35{\cdot}1$ atm^{-1}, $K_B = 5898$ atm^{-1}, $K_C = 23{\cdot}0$ atm^{-1}). The best equation at 40°C was

$$R_A = k\sqrt{(K_B p_A p_B)}/(1 + \sqrt{(K_B p_B)} + \sqrt{(K_C p_C)^4} \qquad (37)$$

($k = 250{\cdot}0$ mol/h kg_{cat}, $K_B = 2{\cdot}3$ atm^{-1}, $K_C = 0{\cdot}067$ atm^{-1}). To determine the activation energy, the constants of the following reaction rate equation were used

$$R_A = k\sqrt{(K_A K_B p_A p_B)}/(1 + \sqrt{(K_A p_A)} + \sqrt{(K_B p_B)} + \sqrt{(K_C p_C)^4} \qquad (38)$$

fitting well in the whole temperature interval covered by the kinetic study (0–40°C). The resulting activation energy was 10·2 kcal/mol; the adsorption enthalpy of hydrogen following from the adsorption coefficients of Eq. (38) was −3·5 kcal/mol. The value for propane was −3·3 kcal/mol.

EXPERIMENTAL

The chemicals and their purification were the same as those in the kinetic study[1,7].

Catalysts pellets. 20 × 20 mm (height × diameter) catalyst pellets were prepared from fine grain catalyst (2% Pd/Al_2O_3) on a hydraulic press. The apparent density of the pellets was 1·987 ± 0·007 g/ml. The size of the catalyst grain prepared for the purposes of the kinetic study[1,7] by crushing the pellets was 0·09 — 0·2 mm. In order to facilitate removal of the pellets from the mould the walls of the mould were treated with ether solution of stearic acid. The surface shell

TABLE I

Physical Properties of the Catalyst

Surface area (BET, adsorption of benzene at 20°C)	163 m^2/g
Apparent density (mercury pycnometry)	1·214 cm^3/g
Density (helium pycnometry)	3·140 cm^3/g
Volume of pores (by adsorption)	0·505 cm^3/g
Porosity (apparent density × pore volume)	0·613 cm^3/cm^3
Macro-pore porosity (pores greater than 100 Å)	0·354 cm^3/cm^3
Effective thermal conductivity (from the limiting temperature difference[8] and cooling curves[9])	$5{\cdot}2 \cdot 10^{-4}$ cal/cm

of the pellets was worked on the lathe to the final dimensions (20·0 ± 0·01) × (20·0 ± 0·01) mm. Physical properties of the catalyst are summarized in Table I. The frequency curve of the pore distribution within 20—800 Å was computed by the Roberts method[10] from the desorption branch of the adsorption isotherm of benzene at 20°C. The pore distribution between 75 and 75000 Å was determined by mercury porosimetry (Carlo Erba Porosimeter, Model 65A). The full frequency curve, obtained by combining both distributions, is shown in Fig. 1. The homogeneity of the prepared pellets was tested by measuring physical properties and catalytic activity of samples taken from various parts of the pellet.

The reduction of pellets was carried out in an auxiliary bath at 200°C in hydrogen (50 ml/min) for 120 hours directly in the reactor designed for measuring reaction rates on the pellets. In contrast to the kinetic region[1,7] the catalytic activity was constant for only about 10 hours. The deactivated pellets could be reactivated by the reduction procedure.

Apparatus. The reaction rates on the catalyst pellets (the effective reaction rates) were measured under atmospheric pressure in a continuous circulating reactor (Fig. 2) under steady state. The reactor was a glass vessel (inner diameter 32 mm) containing the catalyst pellet 10 and connected by spherical ground joints 5 to a circulating pump 3. The temperature of the circulating gas was

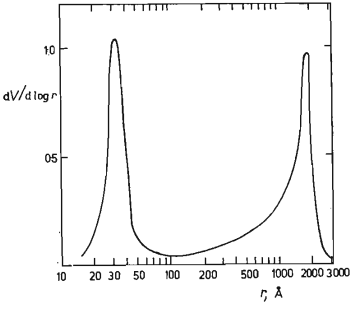

FIG. 1

Frequency Curve of the Pore Size Distribution

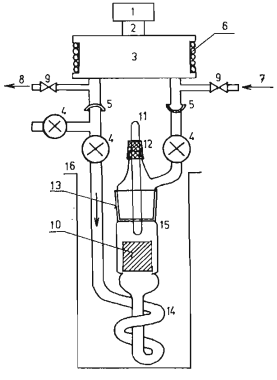

FIG. 2

Differential Circulating Reactor

1 Electromotor, 2 drive, 3 pump, 4 cock, 5 12 mm spherical joint, 6 cooling coil, 7 reaction mixture inlet, 8 reaction mixture outlet, 9 stop valves, 10 catalyst pellet, 11 thermometer, 12 silicon-rubber tube, 13 32/28 mm joint, 14 preheating coil, 15 reactor, 16 bath.

measured by a mercury thermometer 11 the bulb of which reached about 1 cm above the pellet. Glass cocks 4 were used to close the reactor after the reduction of the pellet had been completed and to flush the pump before beginning the kinetic measurements. The glass reactor was submerged in a thermostated bath held at a prescribed temperature. The two-stage pump 3 was made of stainless steel; the balanced rotors were supported on ball bearings. The rotation motion was transmitted by a magnetic clutch consisting of two permanent magnets separated by walls of the circulating pump made of diamagnetic steel. The r.p.m. of the pump could be varied continuously between 2500 and 5000 min^{-1}. Fig. 3 plots the characteristic of the pump (curve *1*) at 4700 r.p.m. used for measurements and for an equimolar mixture of cyclopropane and hydrogen. The operating line of the glass reactor proper (curve 2) intersects the pump characteristic in the operating point corresponding to the rate of circulation of about 20 l/min. Depending on composition of the reaction mixture the rate of circulation ranged between 15 and 25 l/min. The gas components of the reaction mixture were purified and their flow rates measured by capillary flow-meters. The purification of individual components of the reaction mixture as well as the whole mixture was carried out by identical methods as those in the kinetic study of hydrogenolysis of cyclopropane in the kinetic region[1,7]. The chromatographic analysis of the effluent mixture was also the same. In order that we could vary the partial pressures of cyclopropane and hydrogen independently, the reaction mixture was in some experiments diluted by nitrogen before entering the reactor.

The effective reaction rate of cyclopropane was determined from the following equation valid for a perfectly mixed reactor

$$R_{A_{eff}} = (F_A/W)\,X\,. \qquad (39)$$

According to the literature[11–14] a perfectly mixed reactor is one where the ratio of the recycle to the feed rate is greater than about 20. In our case this ratio was equal to several hundreds depending on experimental conditions. The assumption of ideal mixing was tested experimentally by a series of experiments with variable rate of circulation. A part of the experiments is shown in Fig. 4. From the figure it is apparent that at the rate of circulation above 15 l/min the conversion is independent of the circulation rate. This confirms the ideal character of mixing in the reactor, but also the fact that the heat and mass transfer between the bulk of the reactor and the outer surface of the pellets is insignificant. A similar conclusion can be drawn from the experimental finding indicating that the effective reaction rate was not affected by position of the pellet

TABLE II

Binary Diffusion Coefficients $\mathcal{D}_{ij}$ (1 atm) (cm^2/s)

Components *i–j*	20°C	40°C
Cyclopropane–hydrogen	0·464	0·516
Cyclopropane–nitrogen	0·121	0·136
Cyclopropane–propane	0·063	0·072
Hydrogen–nitrogen	0·737	0·825
Hydrogen–propane	0·434	0·489
Propane–nitrogen	0·112	0·135

within the reactor. Owing to the aging the catalyst activity had to be tested by standard experiments. In cases of a minor deactivation the effective reaction rate was corrected computationally on the original activity. Since the activity of individual catalyst pellets was slightly fluctuating, all effective reaction rates were related to the average initial activity of the pellets. The set of the effective reaction rates under standard conditions was used to determine the experimental error: at 20°C the standard deviation amounted to 14% of the average effective reaction rate.

The binary diffusion coefficients of individual pairs of the reacting species were computed from the Hirschfelder equation[15] with the aid of the Lennard-Jones force constants recommended by Satterfield[16]. The results are summarized in Table II.

The Knudsen diffusion coefficients were computed from Eq. (*6*) for the average pore radius 62 Å, following from Wheele's relation[17], and 836 Å, which is an integral mean of the frequency curve from Fig. 1. The diffusion coefficients for cyclopropane in the multicomponent reaction mixture $\mathscr{D}_A$ (or $\mathscr{D}_{As}$) were computed for the same radii from Eq. (*12*). The ratios $\mathscr{D}_A/\mathscr{D}_i$ (or $\mathscr{D}_{As}/\mathscr{D}_{is}$), appearing in the relations for mole fractions (Eqs (*15*), (*17*), see Eq. (*4*)), were evaluated only for the average radius 836 Å since a numerical analysis[7] has revealed their virtual independence on the radius.

The differential mass balance. The mass balance equation derived in the preceding part of this paper assumed an isothermal pellet. The importance of internal heat transfer can be judged[18] for instance from the maximum temperature difference, ΔT_{max}, between the center and the outer surface of the pellet from equation

$$T_{max} = (-\Delta H)\, D_A/c_s\lambda_{eff}\,. \qquad (40)$$

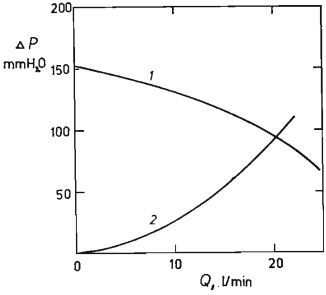

FIG. 3

Pumping Capacity of the Circulating Pump

20°C, 4700 r.p.m., hydrogen–cyclopropane 1 : 1. *1* Pump characteristic, *2* operating line of the reactor.

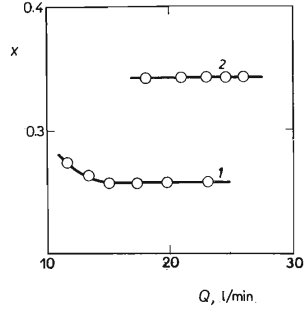

FIG. 4

Cyclopropane Conversion *versus* Rate of Circulation

1 $F_A/W = 12{\cdot}9$ mol/h kg_{cat}, $p_A^0 = p_B^0 = 0{\cdot}5$ atm, *2* $F_A/W = 21{\cdot}52$ mol/h kg_{cat}, $p_A^0 = 0{\cdot}85$ atm, $p_B^0 = 0{\cdot}15$ atm.

It turned out that the maximum temperature difference under our experimental condition was always smaller than 2°C and the heat transfer within the pellet may thus be safely neglected. The choice of the key species was tested for all experimental points according to Eqs (*18*)—(*20*); as the key species was always found cyclopropane (A) even in case of its stoichiometric surplus; (The subscripts must therefore be assigned as follows: $i = 1$ for cyclopropane, (A), $i = 2$ for hydrogen, (B), $i = 3$ for propane, (C)). This is due to the fact that even at a relatively large surplus of hydrogen (B) $\mathscr{D}_{Bs} < \mathscr{D}_{As}$ (see Eq. (*20*)). The expressions for the dimensionless reaction rate appearing in Eq. (*22*) are obtained in the sense of the definition of $f(c)$ from the rate equations (*36*) (20°C) or Eq. (*37*) (40°C) using Eq. (*15*), (model I). When using Eq. (*27*) the mole fractions are given by Eq. (*17*) (model II). The parameter H in case of cyclopropane being a key species is given simply as $H = y_{As}$ (compare Eq. (*24*)). Although the pellet was a cylinder the balance was solved for spherical symmetry ($w = 2$) since according to Aris[5] the solution is expected to differ little from that for a cylinder. For the characteristic dimension l_2 in the modulus M_2 one then can take the radius of a spherical pellet having identical volume-to-outer-surface ratio as the real particle. (In our case this radius equals the radius of the cylinder.) The boundary value problems Eqs (*22*), (*25*), (*26*) (model I), or (*27*), (*25*), (*26*) (model II) were transformed into an initial value problem by the Weisz–Hicks method[19] and integrated numerically on a computer using the Runge–Kutta–Merson technique. The obtained dimensionless concentration gradients on the surface of the pellet, $c'(1)$, were then used to determine the effectiveness factors from Eqs (*28*) or (*29*). In region of strong internal diffusion the effectiveness factors were computed from Eqs (*34*) or (*35*). The trapezoid rule was used for numerical integration combined with Romberg's extrapolation formula[20].

RESULTS AND DISCUSSION

A comparison of the two models of the effect of internal diffusion on the rate of a multicomponent catalytic reaction (model I: Eq. (*22*) together with Eq. (*15*); model II: Eq. (*27*) together with Eq. (*17*)) with the experimental results was based on the effectiveness factor. The values of the effectiveness factors η_{exp}, were obtained

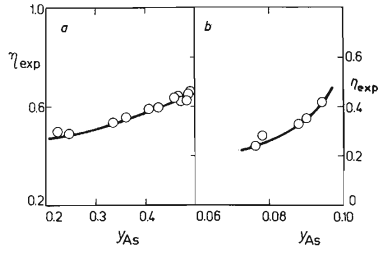

FIG. 5

Effectiveness Factor *versus* Reaction Mixture Composition
a 20°C, $p_A^0 = p_B^0 = 0{\cdot}5$ atm, *b* 40°C, $p_A^0 = 0{\cdot}1$ atm, $p_B^0 = 0{\cdot}9$ atm.

as a ratio of the experimental effective reaction rate to that in the kinetic reagion at concentrations corresponding to those of the reaction mixture surrounding the catalyst pellet. The reaction rates in the kinetic region were computed from Eqs (*36*) (for 20°C) or Eq. (*37*) (40°C). For illustration Fig. 5 plots η_{exp} for two series of experiments at constant hydrogen-to-cyclopropane ratio in the mixture entering the reactor *versus* the degree of conversion. From the figure it is apparent that the effectiveness factor in certain concentration regions depends strongly on composition of the ambient mixture.

Since neither the geometry constant of the catalyst (ε/q), nor the tortuosity (q) (and hence the effective diffusion coefficients D_A) are known, neither the modulus M nor the effectiveness factor can be predicted for a given ambient concentration to test the experimental values of η. To furnish a comparison of the theory with the experiment one thus has to take the opposite procedure, *i.e.* to solve the differential balance and construct the $\eta_2(M_2)$ function for each experimental ambient concentration. The $\eta_2(M_2)$ function then serves to read off the value of the modulus (M_{exp}) corresponding to the experimental effectiveness factor. From the definition of the modulus (Eq. (*23*)) then follows the value of the effective diffusion coefficient D_A, and from Eqs (*4*) and (*12*) the value of the geometry constant ε/q, or q. The effective diffusion coefficients for both models were of the order 10^{-3} cm^2/s and their concentration dependence is shown in Fig. 6 for the same experimental runs as those in Fig. 5. The geometrical constant ε/q can be found for both models of diffusion using $\mathscr{D}_A$ evaluated both for the evarage radius 62 Å and 836 Å. It turns out that in some cases the former value of the average radius leads to $\varepsilon/q > 1$, while for the latter $\varepsilon/q < 1$ in all cases. As it is apparent that the presence of the porous matter causes the effective

TABLE III
ε/q for Average Pore Radius 836 Å

Quantity	Temperature °C	Model I	Model II
Mean value	20	0·118	0·177
	40	0·101	0·127
Variance	20	0·0198	0·0653
	40	0·0085	0·0175
95% Confidence limit (%)[a]	20	55·7	67·3
	40	61·3	69·8

[a] Related to the mean ε/q.

diffusion coefficients to decrease below $\mathscr{D}_A$, the geometrical constants must be smaller than unity. The radius 62 Å may thus be discarded and in the following only 836 Å considered. The average values of ε/q for this radius are summarized in Table III jointly with their variances and 95% confidence limits. As long as the description of internal diffusion is correct all experimental points should provide a single geometrical constant independent of the ambient concentration and temperature with a certain variance owing to the experimental error. From Table III it is seen that model I based on Eq. (2) (*i.e.* on the balance in Eq. (22)) gives somewhat lower estimates of the geometrical constant than model II based on Eq. (3) (*i.e.* on the balance in Eq. (27)). The first of the models displays a better fit to the experiments.

An alternative geometrical characteristics of a porous catalyst is the tortuosity q. In contrast to the constant ε/q, however, one may find several values of the tortuosity for each model of the internal diffusion depending on which porosity ε was used. The porosities which may be possibly used are: the total porosity of the catalyst, ε_t, or the macro-pore porosity, ε_a. The micro-pore porosity was not considered separately since it turned out that for the average pore radius 62 Å the results of ε/q were not consistent. The average tortuosities for the two porosities and model I are summarized in Table IV. Although the tortuosities for ε_a and ε_t are numerically different, their standard deviations are equal. When using ε_t the tortuosity in all experiments was $q > 1$, as expected; for the macro-pore porosity resulted in some cases $q < 1$ which is physically meaningless. The use of the total porosity seems therefore more suitable for calculation of the tortuosity.

The variance of ε/q or the tortuosity may originate in experimental error and from inadequacy of the models of the effect of internal diffusion on the rate of catalytic

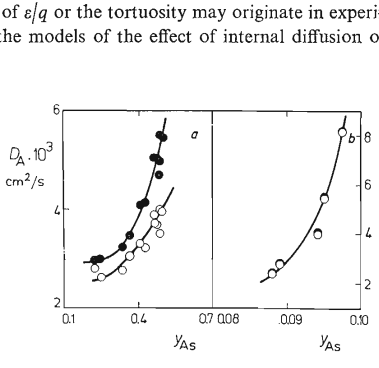

FIG. 6

Effective Diffusion Coefficient of Cyclopropane *versus* Reaction Mixture Composition

a 20°C, $p_A^0 = p_B^0 = 0{\cdot}5$ atm, *b* 40°C, p_A^0 atm $= 0{\cdot}1$, $p_B^0 = 0{\cdot}9$ atm. The points were computed from experimental data and model I (○) or model II (●).

reaction used. While the experimental error caused a random fluctuation around the mean the inadequacy of the model becomes manifest as a systematic deviation of ε/q or q in dependence on composition of ambient mixture. This is manifest in Fig. 7 plotting ε/q *versus* conversion of an equimolar mixture of cyclopropane and hydrogen at 20°C. From the figure it can be further seen that the geometrical constants obtained from model I display a weak concentration trend in contrast to those resulting from model II. Analogous trends displays also the tortuosity. The concentration dependence of ε/q or q remains present at 40°C, too.

The concentration trends cannot be explained unambiguously for the complexity of the problem, but possible reasons are numerous: inadequate description of the multicomponent diffusion, the assumptions of the balance may not be met (*e.g.* the constancy of the total pressure within the pellet), the model of the porous catalyst may not be adequate, or, perhaps, inadequacy of the concentration relations for individual reacting species in a given position within the pellet. Fig. 8 plots the concentrations $y_B(y_A)$ and $y_C(y_A)$ computed from Eqs (*15*) and (*17*) used in models I and II. The figure shows also for comparison some more exact dependences computed by integrating the Stefan–Maxwell equations for the transition region of the diffusion. While $y_B(y_A)$ is not much different, the three approaches provide markedly different courses of $y_C(y_A)$. Since the product of hydrogenolysis – propane – decreases the reaction rate it is clear that an incorrect expression for $y_C(y_A)$ would result in an incorrect prediction of the effectiveness factor, ε/q and q. Since the concentration relations vary with composition of the ambient mixture, the effect will be different

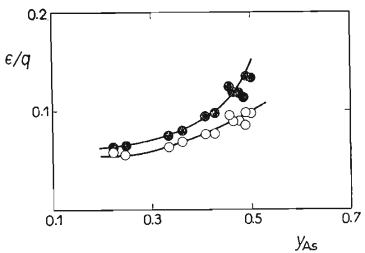

FIG. 7

ε/q versus Reaction Mixture Composition

20°C, $p_A^0 = p_B^0 = 0{\cdot}5$ atm. The points were computed from experimental data and model I (○) or model II (●).

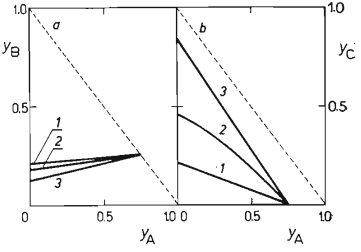

FIG. 8

Concentration Relations

20°C, $p_{As} = 0{\cdot}75$ atm, $p_{Bs} = 0{\cdot}25$ atm. *a* $y_B = y_B(y_A)$, *b* $y_C = y_C(y_A)$ *1* Eq. (*17*), *2* Eq. (*15*), *3* The Stefan–Maxwell equation for transition region of diffusion.

TABLE IV
Tortuosity for Average Pore Radius 836 Å and Model I

Quantity	Temperature °C	For ε_t	For ε_a
Mean value	20	11·6	6·7
	40	11·4	6·2
Variance	20	100·4	33·4
	40	63·7	19·0
95% Confidence limit (%)[a]	20	40·3	40·2
	40	47·0	46·9

[a] Related to the mean q.

in various concentration ranges which in turn may give rise to concentration trends of the geometrical constant. In this connection the question becomes that of the accuracy of determining the adsorption coefficient K_C, which, unlike those of cyclopropane and hydrogen, was determined from a smaller number of experimental data[1,7].

The relation between the scatter of the experimental geometrical constant and the deviation of the experimental and theoretical effectiveness factor could not be estimated in advance. For illustration we have therefore computed the mean deviation for model I and the pore radius 836 Å using ε/q from Table III. At 20°C the deviation amounted to 0·12 (units of effectiveness factor), *i.e.* 20% rel., at 40°C 0·10, *i.e.* 23% rel. It is natural that the concentration trends of the geometrical constant bring about analogous trends in the deviations of the experimental and predicted effectiveness factors.

LIST OF SYMBOLS

a_i	relative stoichiometric coefficient
a	change of mole number due to reaction, Eq. (*13*)
A_i	reaction mixture component (reacting species $i = 1, \ldots, p$; inerts $i = q, \ldots, n$)
c_T	total concentration of gas mixture
c	dimensionless concentration of key species in porous pellet
$\mathscr{D}_i$	diffusion coefficient of A_i in multicomponent reaction mixture
$\mathscr{D}_{ij}$	binary diffusion coefficient of pair A_i—A_j
$\mathscr{D}_{ki}$	Knudsen diffusion coefficient of A_i
D_i	effective diffusion coefficient of A_i in multicomponent reaction mixture
$f(c)$	dimensionless reaction rate

F_A	feed rate of cyclopropane
ΔH	reaction enthalpy
H	parameter, Eq. (*24*)
k	reaction rate constant
K_i	adsorption coefficient of A_i
l_w	characteristic dimension of the catalyst pellet
M_w	Thiele modulus, Eq. (*23*)
N_i	molar diffusion flux of A_i related to unit area of cross-section of porous pellet
p_i	partial pressure of A_i
p_i^0	inlet partial pressure
q	tortuosity
r	pore radius
R_i	reaction rate of A_i per unit volume of catalyst pellet
$R_{A,eff}$	effective reaction rate of cyclopropane
ΔT_{max}	maximum temperature difference in the pellet
v_i	thermal velocity of molecules A_i
$v = M_w(1 - x)$	transformed coordinate
w	geometrical coefficient (infinite slab $w = 0$, infinite cylinder $w = 1$, sphere $w = 2$)
W	volume of pellet
x	dimensionless coordinate
X	conversion of cyclopropane
y_i	mole fraction of A_i
z	coordinate
α_i	stoichiometric coefficient of A_i($\alpha_i > 0$ for products, $\alpha_i < 0$ for reactants)
ε	porosity
ε_t	total porosity
ε_a	macro-pore porosity
λ_{eff}	effective thermal conductivity of pellet
η_w	effectiveness factor for geometry w
η_w^*	effectiveness factor in region of strong internal diffusion

Subscripts

i	reacting species
A	cyclopropane
B	hydrogen
C	propane

REFERENCES

1. Antl L., Schneider P.: This Journal *38*, 2408 (1973).
2. Butt J. B.: Can. J. Chem. Eng. *9*, 130 (1963).
3. Cunningham R. S., Geankoplis C. J.: Ind. Eng. Chem. Fund. *2*, 429 (1968).
4. Evans R. B., Watson G. M., Mason E. A.: J. Chem. Phys. *33*, 2076 (1961).
5. Kubota H., Yamanaka Y., Dalla Lana J. G.: J. Chem. Eng. Japan *2*, 71 (1969).
6. Weekman V. W., Gorring R. L.: J. Catal. *4*, 260 (1965).
7. Antl L.: *Thesis*. Czechoslovak Academy of Sciences, Prague 1972.
8. Jirátová K.: *Thesis*. Institute of Chemical Technology, Prague 1967.

9. Mejstříková M., Horák J.: Chem. průmysl *22/47*, 61 (1972).
10. Roberts B. F.: J. Colloid Inter. Sci. *23*, 266 (1967).
11. Carberry J. J.: Catal. Rev. *3*, 61 (1970).
12. Rudkin J.: Brit. Chem. Eng. *12*, 1347 (1967).
13. Temkin M. J.: Kinetika i Kataliz *3*, 509 (1962).
14. Vosolsobě J., Michálek J.: This Journal *31*, 2646 (1966).
15. Bird R. B., Stewart W. E., Lightfoot E. N.: *Transport Phenomena.* Wiley, New York 1960.
16. Sattereld C. N.: *Mass Transfer in Heterogeneous Catalysis.* MIT Press, Massachusetts, USA 1970.
17. Wheeler A.: Advan. Catal. *2*, 105 (1955).
18. Damköhler G.: Z. Physik. Chem. (Leipzig) *A 193*, 16 (1943).
19. Weisz P. B., Hicks J. S.: Chem. Eng. Sci. *17*, 265 (1962).
20. Filippi S.: Math. Tech.-Wirtschaft *11*, No 2, 49 (1964).

Translated by V. Staněk.